JOURNAL OF BACTERIOLOGY, Dec. 1989, p. 6680–6688
0021-9193/89/126680-09$02.00/0

Vol. 171, No. 12

Erythromycin-Induced Ribosome Stall in the *ermA* Leader: a Barricade to 5′-to-3′ Nucleolytic Cleavage of the *ermA* Transcript

PAULA SANDLER[1] AND BERNARD WEISBLUM[2]*

Department of Pharmacology, University of Wisconsin Medical School,[2] and Department of Genetics, University of Wisconsin,[1] Madison, Wisconsin 53706

Received 15 June 1989/Accepted 8 September 1989

The *Staphylococcus aureus ermA* gene, whose product confers resistance to the macrolide-lincosamide-streptogramin B family of antibiotics, is induced at the level of translation by nanomolar concentrations of erythromycin. Erythromycin also specifically stabilizes *ermA* transcripts, and the induced stabilization requires in-phase translation of at least one of two small leader peptides in the 5′ leader region of the transcript. Erythromycin-induced mRNA stabilization was tested in three constructions in which the *ermA* transcript was elongated by making insertions at the *ermA* transcription start. Whereas mRNA downstream of the leader peptide is stabilized by erythromycin, mRNA upstream is not. In the presence of erythromycin, specific mRNA decay intermediates in both the extended *ermA* genes and the wild-type *ermA* gene were detected by both Northern blotting and S1 nuclease mapping. The 5′ ends of the intermediates map to the sequences that encode each of the two *ermA* leader peptides, suggesting that the intermediates are produced by stalled erythromycin-bound ribosomes acting as barricades to degradation by 5′-to-3′ RNases. In addition, whereas erythromycin was found previously to stabilize *ermA* transcripts only physically, an *ermC–cat-86* hybrid transcript was stabilized both physically and functionally by erythromycin.

The stability of procaryotic mRNAs varies widely, leading to differential rates of gene expression (for reviews, see references 4 and 7). Several enzymes that can participate in the degradation of mRNAs have been identified, and various sequence determinants and structural features of transcripts have been shown to influence the rates of decay of specific transcripts. Our studies have focused on antibiotic-induced stabilization of transcripts of the *erm* family of genes from *Staphylococcus aureus*.

The *erm* family of genes specifies rRNA methylases that confer resistance to macrolide, lincosamide, and streptogramin B antibiotics by reducing the affinity between these antibiotics and ribosomes. Expression of the methylase is induced by nanomolar concentrations of the macrolide antibiotic erythromycin (28). Genetic and biochemical studies of *S. aureus* gene *ermC*, a model system for erythromycin-induced antibiotic resistance, have demonstrated that synthesis of rRNA methylase is posttranscriptionally controlled by a translational attenuation mechanism (14, 16). According to the translational attenuation model, *ermC* mRNA is transcribed constitutively, but only low levels of methylase protein are synthesized because the ribosome-binding site and initiation codon for the methylase are sequestered by mRNA secondary structure. In the presence of erythromycin, the antibiotic-bound ribosomes stall while translating a 19-amino-acid leader peptide located near the 5′ end of the *ermC* transcript. The stalled ribosomes effect a conformational change in the secondary structure of the transcript that frees the previously base-paired methylase translation initiation sequences, resulting in an increased rate of methylase synthesis.

S. aureus gene *ermA* is regulated by a translational attenuation mechanism similar to that of *ermC* (23); however, in contrast to that of *ermC*, the *ermA* leader can assume a more complex structure and encodes two peptides (15 and 19 amino acids long; see Fig. 1a). Induction of *ermA* is thought to require two successive ribosome-stalling events. Erythromycin-bound ribosomes that stall while translating the first leader peptide free the translation start signals for the second leader peptide, and erythromycin-bound ribosomes that stall while translating the second leader peptide, in turn, free the *ermA* methylase translation start signals (23).

Nanomolar concentrations of erythromycin also specifically increase the half-life of *erm* mRNA 7- to 20-fold in *S. aureus* or *Bacillus subtilis* (3, 26). Previous reports have proposed that the induced stabilization is due to stalling of erythromycin-bound ribosomes as they translate specific amino acid codons of the *erm* leader peptides; replacing the second codon of the *ermC* leader peptide with a stop codon or creating a frameshift in the first *ermA* leader peptide eliminates the induced stabilization (3, 26). Moreover, gene fusion experiments have demonstrated that just the 5′ end of *ermA* or *ermC*, including the leader peptide and part of the methylase-coding region, fused to the *E. coli lacZ* gene suffices to confer increased stabilization on the hybrid transcript (3, 26). Although the *ermA-lacZ* transcript was physically stabilized in the presence of erythromycin, the transcript did not appear to be functionally stabilized (26).

Because sequences that encode the *ermA* and *ermC* leader peptides are located less than 25 nucleotides (nt) downstream from the +1 sites of their respective transcripts, an erythromycin-bound ribosome that stalls while translating the leader peptides could shield almost the entire 5′ end of the message. This finding suggested that stalled ribosomes might, as a result, stabilize *erm* transcripts by limiting the accessibility of RNases that bind at the 5′ end of the message. To test this model, we inserted sequences in the *ermA* leader region that increased the distance between the +1 site and the first leader peptide and monitored the decay of the resultant elongated transcripts. We found that although erythromycin induced stabilization of mRNA downstream of the leader peptide sequences, the inserted mRNA upstream was not stabilized unless an additional leader peptide sequence was inserted 5′ to the extension. These

* Corresponding author.

TABLE 1. Strains and plasmids

Strain or plasmid	Description or derivative	Reference
Strains		
B. subtilis PSL-1	Transformable host lacking restriction	25
E. coli NM522	Transformable host lacking restriction	13
Plasmids		
pBS42	*E. coli-B. subtilis* shuttle vector	2
pLS463	*ermA* from *S. aureus* 1206 (*Fnu*4HI + *Bam*HI-*Eco*RI linker, cut with *Eco*RI) ligated into pBS42 (*Eco*RI)	26
pLS201	From pLS463 by in vitro mutagenesis of *ermA*, yielding *ermA201* (*ermA* with *Hpa*I site at mRNA +1 site)	This work
pE194	*S. aureus* plasmid containing *ermC* gene	17
pC194	*S. aureus* plasmid containing *cat* gene	18
pLS202	pLS201 (*Hpa*I) + 407-bp *Dra*I fragment, bp 2474–bp 2067 of pE194, yielding *ermA202*	This work
pLS217	pLS201 (*Hpa*I) + 434 bp, from *Stu*I at bp 1885 to *Alu*I site at bp 1451 of pC194, yielding *ermA217*	This work
pLS212	pLS201 (*Hpa*I) + 719 bp *Hinf*I fragment C, from bp 3538 to bp 526 of pE194 (filled in), yielding *ermA212*	This work
pLS238	pLS201 (*Hpa*I) + 101 bp, from *Hpa*I to *Rsa*I at bp 100 of *ermA201* (on plasmid pLS201) + same *Dra*I fragment as pLS202, yielding *ermA238*	This work
pPL603B	*B. subtilis* vector containing promoterless *cat-86*, derived from pPL603 by insertion of *Bam*HI adaptor into *Eco*RI site	29
pLS767	pPL603B (*Bam*HI) + 355 bp, from *Hpa*II at bp 3137 to *Hinf*I at bp 2782 of pE194	This work

results and detection of specific mRNA decay intermediates that map to the *ermA* leader peptides suggest that erythromycin-bound ribosomes block the progression of a 5′-to-3′ processive RNase.

MATERIALS AND METHODS

Bacterial strains. The strains used are described in Table 1.

Plasmid constructions. The plasmids used in this study are described in Table 1. The 19-mer oligonucleotide 5′-ATTCAGTTAACATAAGGAG-3′ served as a mutagenic primer (31) for introduction of an *Hpa*I site at +1 into plasmid pLS463. The resultant plasmid, pLS201, was used as the host for insertion of extensions to the *ermA* transcript.

RNA isolation. Erythromycin at 30 ng/ml (40.8 nM) was added to cultures of *B. subtilis* growing exponentially at 37°C in L broth. After 15 min, rifampin (Sigma Chemical Co.) at 150 μg/ml was added and cells were harvested at the times indicated for extraction of total cellular RNA as previously described (26).

Northern (RNA) blot analysis. RNA transcript stabilization was analyzed by Northern blot analysis as previously described (26). The *ermA* probe consisted of the 1,400-base-pair (bp) *Eco*RI *ermA* fragment from plasmid pLS463. The *cat-86* probe consisted of the 412-bp *Hpa*I-*Hin*dIII fragment internal to the *cat-86* coding region from plasmid pPL603B. Both probes were uniformly ^{32}P labeled by the oligolabeling procedure of Feinberg and Vogelstein (11) to a specific activity of 1×10^8 to 3×10^8 cpm/μg.

S1 nuclease mapping. The DNA fragments for use as probes in S1 nuclease mapping experiments were the 840-bp *Hinf*I-*Eco*RI fragment from pLS202, the 1,150-bp *Hinf*I-*Eco*RI fragment of pLS212, and the 1,025-bp *Dde*I-*Eco*RI fragment of pLS217. T4 polynucleotide kinase (New England BioLabs, Inc.) was used to label the *Hinf*I or *Dde*I ends with [γ-^{32}P]dATP (Dupont, NEN Research Products). Mapping of transcripts with S1 nuclease was performed as described by Berk and Sharp (6). Total cellular RNA (2 μg) was hybridized at 40°C with the end-labeled probes, digested with S1 nuclease (500 U/ml; Sigma), ethanol precipitated, and fractionated on 8 M urea–6% polyacrylamide gels. The specific activity of the DNA probes was 1×10^5 to 5×10^5 (Cherenkov counts)/min per μg.

CAT assays. Chloramphenicol acetyltransferase (CAT) activity was assayed at 37°C by the spectrophotometric method described by Shaw (27). The specific activity of CAT is reported as micromoles of chloramphenicol acetylated per minute per milligram of protein.

RESULTS

Decay of extended *ermA* transcripts. We have previously shown that in-phase translation of *ermA* leader peptide 1, located near the 5′ end of the transcript (Fig. 1), is required for erythromycin-induced stabilization of the *ermA* transcript (26). To determine whether proximity of the leader peptide to the 5′ end of the transcript plays a role in the induced stabilization, we monitored the decay of *ermA* transcripts containing extensions that were added upstream of leader peptide 1. The wild-type *ermA* gene had been previously subcloned to an *Escherichia coli-B. subtilis* shuttle vector (plasmid pLS463; 26), and to construct the *ermA* extensions for the present study, an *Hpa*I recognition sequence was introduced at the transcriptional +1 site of *ermA*. The resultant plasmid construct was designated pLS201, and the *ermA* allele was correspondingly named *ermA201* (Fig. 2); throughout this report, the same number is assigned to both the *ermA* allele and the plasmid that carries it. Each of the extended *ermA* genes was constructed by cloning restriction fragments into the *Hpa*I site of pLS201 (Fig. 2). The restriction fragments used comprised internal segments from known *S. aureus* plasmid open reading frames, reducing the chance that they contain transcription or translation start signals.

Decay of transcripts from the extended *ermA* gene *ermA202*, which contains a 407-bp *Dra*I restriction fragment internal to the coding region of *S. aureus ermC*, was characterized by Northern blot analysis. *B. subtilis* PSL-1 cells containing plasmid pLS202 were induced with erythromycin. Rifampin was added to halt further transcription initiation, and cells were harvested at the times indicated (Fig. 3a). RNA purified from each sample was separated by electrophoresis on a 1% agarose–formaldehyde gel, blotted to nitrocellulose, and hybridized with a uniformly labeled *ermA*-specific probe. A band corresponding to the extended *ermA* transcript (labeled A in Fig. 3a) was detected at time

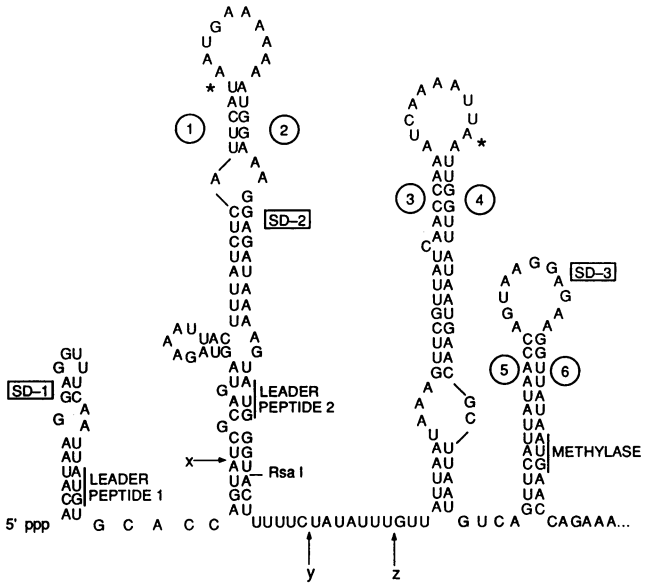

FIG. 1. Nucleotide sequence of the *ermA* control region. The nucleotide sequence and proposed secondary structure of the *ermA* mRNA control region, as reported by Murphy (23), are shown. Translation of the two leader peptides begins at leader peptides 1 and 2, and the translation stops are indicated by asterisks. The translation start codon of the methylase is also shown. The 5′ endpoints of cleavage products x, y, and z are indicated by arrows. SD-1 to SD-3 are ribosome-binding sites. The circled numbers indicate the six stem segments that comprise the *ermA* control region.

zero both with and without erythromycin (lanes 2 and 7). Additionally, a truncated transcript (labeled B) was detected in the RNA samples isolated from erythromycin-induced cells (lanes 7 to 11). The length of this shorter transcript corresponded in size to the wild-type *ermA* transcript (cf.

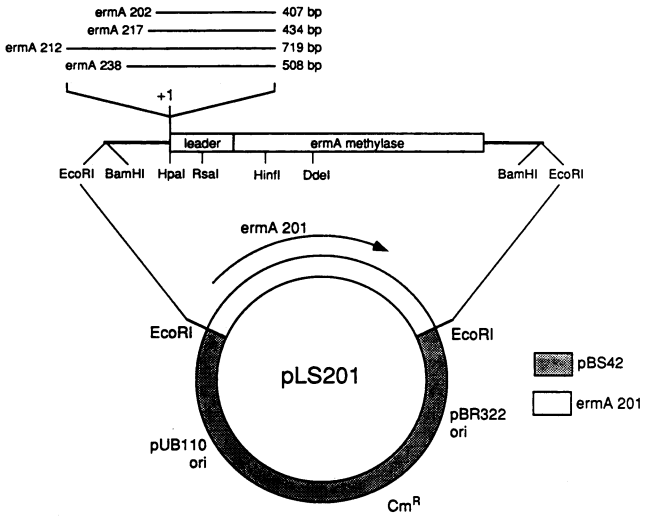

FIG. 2. Diagram of plasmid pLS201. The plasmid, based on pBS42 (2), contains the pC194 chloramphenicol resistance (Cm^R) gene, replication functions for both *E. coli* and *B. subtilis*, and *ermA201* (*ermA* with an *Hpa*I restriction site introduced at the transcriptional +1 site). A physical map of *ermA201* is shown with relevant restriction sites. The sizes of four insertions at the *Hpa*I site, resulting in *ermA202*, *ermA217*, *ermA212*, and *ermA238*, are indicated. ori, Origin of replication.

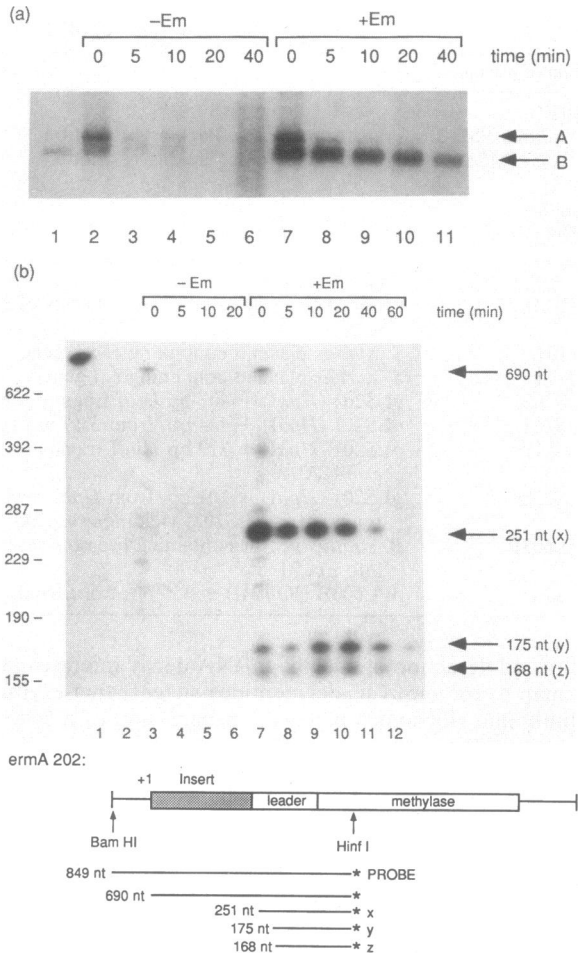

FIG. 3. Decay of *ermA202* mRNA. Total RNA was isolated from erythromycin (Em)-induced and uninduced cultures of *B. subtilis* PSL-1(pLS202) at the times indicated after addition of rifampin. (a) Northern blot analysis. RNA was fractionated, blotted, and probed with an *ermA*-specific probe. Lane 1 contains RNA from *B. subtilis* PSL-1 carrying pLS463, a plasmid with the wild-type *ermA* gene, isolated immediately after rifampin addition without erythromycin induction. A and B indicate extended- and truncated-transcript mobilities, respectively. (b) S1 nuclease analysis. Total RNA from panel was annealed with an 849-nt probe that was ^{32}P 5′ end labeled at the *Hin*fI site as shown. Lanes: 1, probe not digested with S1 nuclease; 2, 2 μg of *E. coli* tRNA; 3 to 12, 2 μg of total cellular RNA. Molecular sizes of markers are shown on the left in nucleotides.

lane 1 with band B in lanes 7 to 11). With erythromycin, the half-life of the extended transcript (band A) was short ($t_{1/2}$ <2 min) compared with that of the truncated transcript (band B), whose half-life is approximately 15 min.

The 5′ endpoints of the two *ermA202* transcripts detected by Northern blot analysis were determined by S1 nuclease mapping. Total cellular RNA prepared from cells treated as for Fig. 3a was hybridized with a 5′-end-labeled *Hin*fI probe (Fig. 3b). Samples were digested with S1 nuclease, and the protected fragments were resolved on an 8 M urea–6% polyacrylamide gel. Protected DNA fragments corresponding to the full-length extended *ermA* transcript (690 nt) were detected at comparable intensities in the zero-time samples obtained both with and without erythromycin (lanes 3 and 7). Additionally, three smaller DNA fragments (labeled x, y, and z in Fig. 3b) were detected only in samples that received erythromycin. These bands, corresponding to transcripts

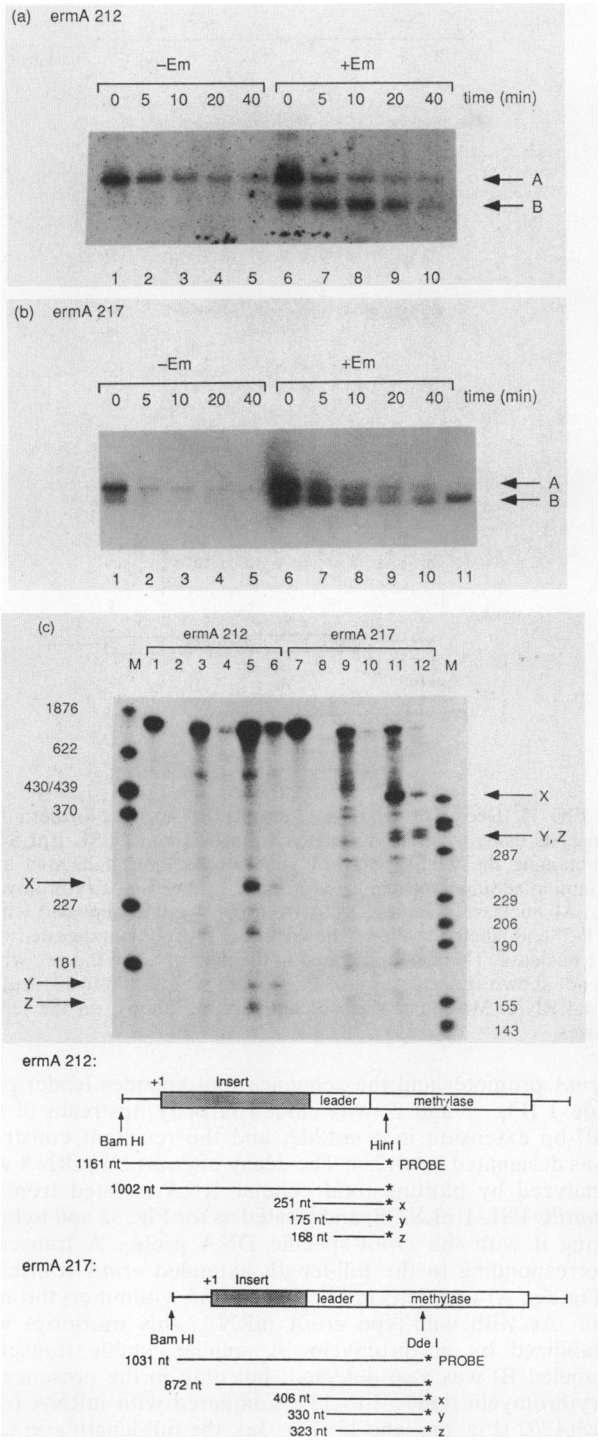

FIG. 4. Decay of *ermA212* and *ermA217* mRNAs. (a) and (b) Northern blot analysis using total RNA, prepared as for Fig. 2, from *B. subtilis* PSL-1 containing plasmid (a) pLS212 or (b) pLS217, hybridized with an *ermA*-specific probe. A and B indicate extended- and truncated-transcript mobilities, respectively. Lane 11 (b) contains RNA from *B. subtilis* PSL-1(pLS463) (wild-type *ermA*) isolated at time zero after rifampin addition without erythromycin (Em) induction. (c) S1 nuclease analysis. Total RNA isolated from uninduced and erythromycin-induced cultures of *B. subtilis* PSL-1 carrying pLS212 or pLS217 was annealed with either a *Hin*fI (for pLS212) or a *Dde*I (for pLS217) ^{32}P-5′-end-labeled probe as shown. Lanes: 1 and 7, *Hin*fI or *Dde*I probe, respectively, not digested with S1 nuclease; 2 and 8, 2 μg of *E. coli* tRNA; 3 to 6, 2 μg of total RNA from cells carrying pLS212 isolated immediately (lanes 3 and 5) or 30 min (lanes 4 and 6) after rifampin addition with or without erythromycin induction, as shown; 9 to 12, 2 μg of total RNA from cells carrying pLS217 isolated immediately (lanes 9 and 11) or 30 min (lanes 10 and 12) after rifampin addition with or without erythromycin induction, as shown. Molecular sizes of markers are shown on both sides in bases.

with differing 5′ ends, were not resolved by the Northern blot experiment described above (Fig. 3a); transcript B (Fig. 3a) was composed of a combination of transcripts which correspond to fragments x, y, and z. Consistent with other S1 nuclease experiments, bands y and z accumulated with time (Fig. 3b), suggesting a precursor-product relationship with respect to the larger erythromycin-stabilized band (labeled x) as the precursor. Further resolution of these S1 nuclease-resistant fragments on an 8 M urea–6% polyacrylamide sequencing gel (data not shown) revealed that the mRNA 5′ termini corresponding to DNA fragments x (251 nt), y (175 nt), and z (168 nt) each mapped to the *ermA* leader region (Fig. 1). Band x corresponds to an *ermA* transcript cleaved in codon 5 of the first leader peptide, whereas bands y and z correspond to *ermA* transcripts cleaved in codon 5 and after codon 7 of the second leader peptide, respectively.

Transcripts x, y, and z detected in the presence of erythromycin could represent, in principle, either decay intermediates or new transcriptional starts. The former is more likely because the smaller bands accumulated at later times after rifampin addition. Moreover, the same erythromycin-induced bands appeared, irrespective of the composition of the inserted DNA sequence (see below).

To test the generality of the results obtained with *ermA202*, we analyzed the decay patterns of mRNA from two additional extended *ermA* genes. Plasmid pLS212 contains *ermA* with a 719-bp *Hin*fI restriction fragment internal to the coding region of open reading frame A of plasmid pE194 (17), and pLS217 contains *ermA* with a 434-bp *Stu*I-*Alu*I restriction fragment internal to the *cat* gene of plasmid pC194 (18). Both restriction fragments were inserted at the *Hpa*I site of *ermA201* (Fig. 2). Blots of total cellular RNA from *B. subtilis* PSL-1(pLS212) and *B. subtilis* PSL-1(pLS217) prepared as for *ermA202* (Fig. 3a) were hybridized with the *ermA*-specific probe, and the results are shown in Fig. 4a and b. For both constructions, a band corresponding to the full-length extended *ermA* transcript was detected both without and with erythromycin (labeled band A). With erythromycin, (Fig. 4a and b, lanes 6 to 10), a truncated transcript close in size to the wild-type *ermA* transcript (Fig. 4b, lane 11) was found (band B). The truncated transcripts were stable (half-lives of approximately 15 min) compared with the full-length extended transcripts, which decayed with half-lives of less than 2 min both with and without erythromycin. These results are similar to those obtained with *ermA202* (Fig. 3a).

The decay of the *ermA212* and *ermA217* transcripts was further characterized by S1 nuclease mapping as described above, with RNA from *B. subtilis* PSL-1 containing either pLS212 or pLS217 and 5′-end-labeled probes (Fig. 4c). S1-resistant fragments were resolved on an 8 M urea–6% polyacrylamide gel (Fig. 4c). As with *ermA202*, besides the full-length *ermA212* and *ermA217* transcripts, specific decay intermediates (labeled x, y, and z) were detected in the presence of erythromycin (Fig. 4c). For *ermA212*, bands x, y, and z appeared in lanes 5 and 6 and for *ermA217*, bands x, y, and z appeared in lanes 11 and 12. The *ermA212* and

ermA217 decay intermediates correspond in size to those which appeared with *ermA202* as described above, and thus, these intermediates also map to the sequence that encodes the *ermA* leader peptides. Increasing the distance between the 5′ end of the transcript and leader peptide 1, therefore, had the same effect on all three extended *ermA* transcripts: the mRNA downstream from the leader peptides was stabilized by erythromycin, while the inserted upstream mRNA was not.

Decay of the wild-type *ermA* transcript. Studies of the decay of *ermA202*, *ermA212*, and *ermA217* transcripts showed several mRNA decay intermediates with 5′ termini that map to the sequence that encodes the leader peptides. Our previous studies (26) showing enhanced stability of the full-length wild-type *ermA* transcript by S1 nuclease mapping were not optimized to detect such intermediates because of the use of a DNA probe whose 5′ terminus mapped to the *ermA* leader region. To determine whether decay of the wild-type transcript produces these intermediates, we reexamined the pattern of decay of the wild-type *ermA* transcript by using a DNA probe labeled at the *Hin*fI site internal to the *ermA* coding region.

The decay pattern of the wild-type *ermA* transcript was analyzed by Northern blotting. Total cellular RNA from *B. subtilis* PSL-1 carrying plasmid pLS463, a plasmid with the wild-type *ermA* gene, was probed with the *ermA*-specific probe. A single *ermA* transcript was detected (Fig. 5a). The half-life of the transcript increased from less than 2 min to 20 min with erythromycin induction.

Decay of the wild-type transcript was analyzed further by S1 nuclease mapping. Total cellular RNA prepared from *B. subtilis* PSL-1(pLS463) cells treated as for Fig. 3a was hybridized with a DNA probe that had been 5′ end labeled at the *Hin*fI site (Fig. 5b), and the resultant hybrids were digested with S1 nuclease. The protected fragments were separated on an 8 M urea–6% polyacrylamide gel, and the results are shown in Fig. 5b. A band corresponding to the full-length *ermA* transcript (283 nt) was detected with and without erythromycin. In contrast to the full-length extended *ermA* transcripts examined above, this full-length wild-type transcript was stabilized by erythromycin (increase in $t_{1/2}$ from 2 to about 20 min). The S1 nuclease-resistant DNA fragments x, y, and z identified for the extended *ermA* mRNAs were also found for the wild-type *ermA* mRNA (Fig. 5b, lanes 8 to 13), suggesting that these intermediates are not a consequence of extension of the *ermA* transcript. The ratio of the level of decay intermediates to that of the full-length transcript, however, was less with the wild-type *ermA* transcript than with the extended transcripts.

Decay of the *ermA* transcript in a 5′-to-3′ direction from the 5′ end. The finding that decay intermediates were relatively more abundant in the decay of extended versus wild-type transcripts suggests that the extensions contribute to transcript decay. The extensions may contribute binding sites for endonucleases, free ends for exonuclease degradation, or possibly both. To distinguish among the possibilities, we capped one of the extended transcripts with the sequence that encodes leader peptide 1. If the *ermA* transcript were subjected to endonucleolytic cleavage, we would not expect capping of the extension with an additional leader to change the decay pattern of the transcript. If, on the other hand, decay were by an exonuclease, adding a ribosome stall site to the 5′ end of the transcript may stabilize the entire transcript by preventing the enzyme from binding to its substrate.

A 101-bp *Eco*RI-*Rsa*I restriction fragment containing the

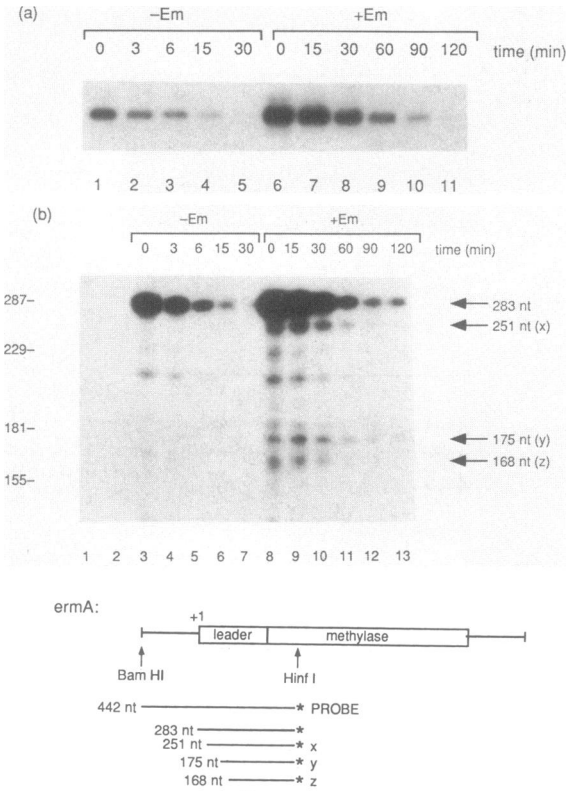

FIG. 5. Decay of wild-type *ermA* mRNA. (a) Northern blot analysis using total RNA isolated from *B. subtilis* PSL-1(pLS463) containing the wild-type *ermA* gene at the times indicated after rifampin addition with an *ermA*-specific probe. Em, Erythromycin. (b) S1 nuclease mapping. RNA from panel a was annealed with a ^{32}P-5′-end-labeled probe as shown. Lane 1, probe not digested with S1 nuclease. The probe migrated in the upper part of the gel, which is not shown. Lane 2, 2 μg of *E. coli* tRNA. Lanes 3 to 13, 2 μg of total RNA. Molecular sizes of markers are shown on the left in bases.

ermA promoter and the sequence that encodes leader peptide 1 (Fig. 1 and 2) was cloned directly upstream of the 407-bp extension in *ermA202*, and the resultant construct was designated *ermA238*. The decay of *ermA238* mRNA was analyzed by blotting total cellular RNA isolated from *B. subtilis* PSL-1(pLS238) and treated as for Fig. 3a and hybridizing it with the *ermA*-specific DNA probe. A transcript corresponding to the full-length extended *ermA* transcript (Fig. 6a, A) was detected both with and without erythromycin. As with wild-type *ermA* mRNA, this transcript was stabilized by erythromycin. A smaller, stable transcript (labeled B) was also detected, but only in the presence of erythromycin (lanes 7 to 12). Compared with mRNA from *ermA202* (Fig. 6a, lane 13; Fig. 3a), the full-length *ermA238* transcript (band A) was more stable with erythromycin. These results are consistent with a model of processive decay from the 5′ end of the transcript rather than endonucleolytic cleavages in the *ermA* leader peptide.

Results consistent with the Northern blot experiment (Fig. 6a) were obtained by S1 nuclease mapping (Fig. 6b). The 791-nt DNA fragment which corresponds to the full-length *ermA238* transcript decayed rapidly without erythromycin (lanes 3 to 5) but was stabilized by erythromycin (lanes 6 to 10). DNA fragments corresponding to intermediates x, y, and z were detected in the presence of erythromycin, but at low levels compared with the full-length transcript.

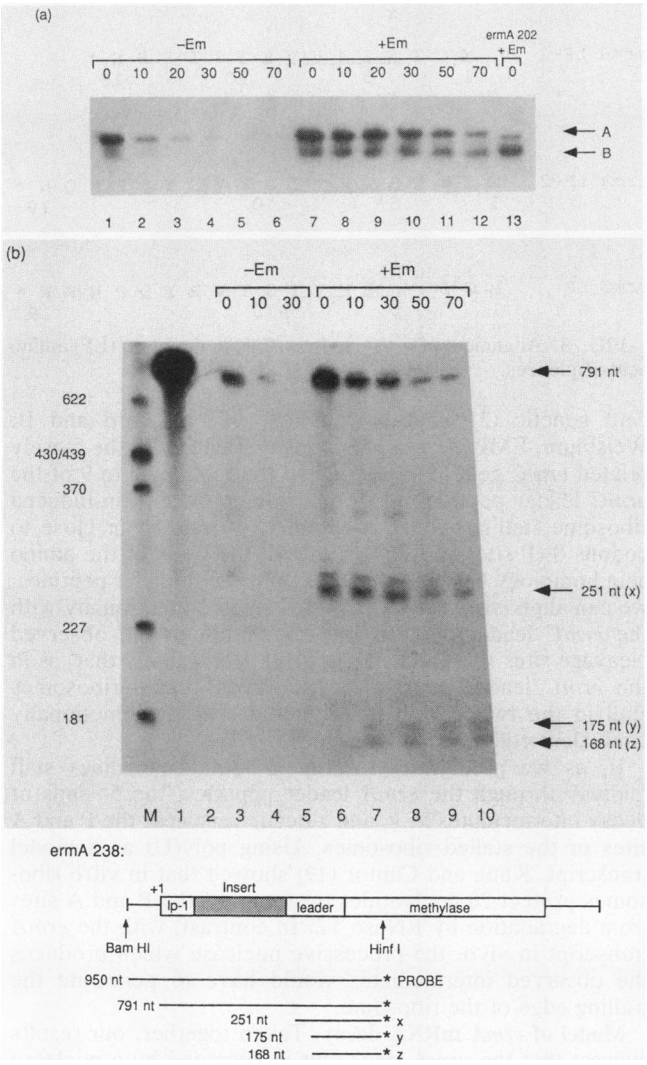

FIG. 6. Decay of *ermA238* mRNA. (a) Northern blot analysis using total RNA isolated from *B. subtilis* PSL-1(pLS238) at the times indicated after rifampin addition with an *ermA*-specific probe. Lane 13 contained RNA from erythromycin (Em)-induced cells carrying plasmid pLS202 isolated at time zero after rifampin addition. (b) S1 nuclease mapping. RNA from panel a was annealed with a ^{32}P-5′-end-labeled *Hin*fI probe as shown. Lanes: 1, probe not digested with S1 nuclease; 2, 2 μg of *E. coli* tRNA; 4 to 10, 2 μg of total cellular RNA. Molecular sizes of markers are shown on the left in bases.

Stabilization of the *cat-86* transcript both physically and functionally by the *ermC* leader peptide sequence. According to the results described above, the mRNA downstream from the *ermA* control region is stabilized by erythromycin. This suggests that the internal region of the *ermA* transcript and the 3′ end are relatively resistant to nuclease attack. The same must be true for the *E. coli lacZ* transcript, as the 5′ end of either *ermA* or *ermC* fused to the 3′ end of *lacZ* stabilizes the entire hybrid transcript (3, 26). As part of a survey to correlate physical and functional stabilization of mRNAs, we tested the ability of the 5′ end of *ermC* to stabilize *cat-86* from *B. pumilus* (15). *ermC* was used because of the ease with which it is possible to obtain a promoter-leader peptide cassette by digestion of pE194 DNA with *Hpa*II and *Hin*fI. A 355-bp DNA fragment

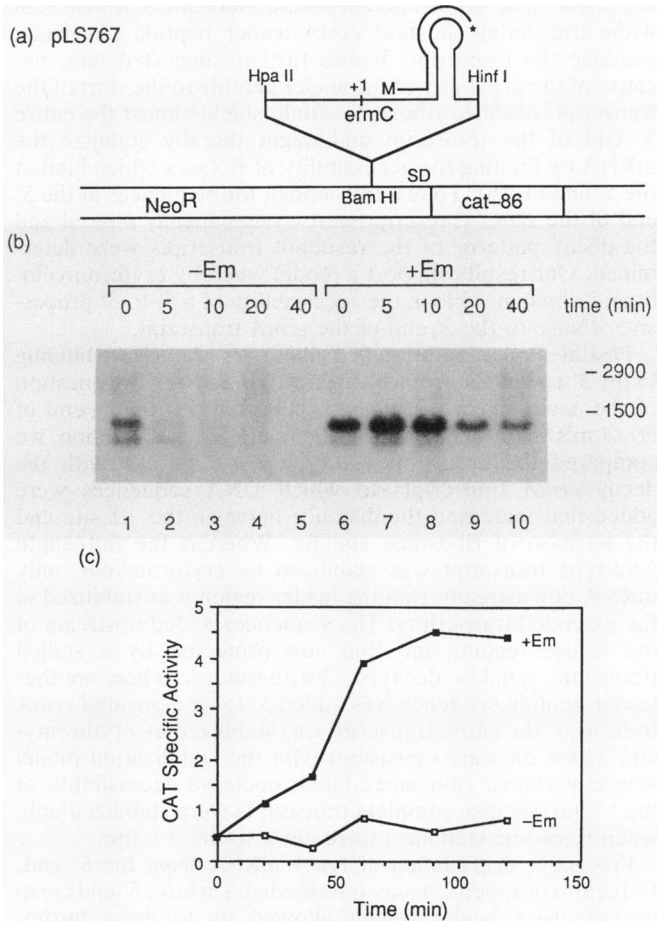

FIG. 7. Erythromycin (Em)-induced chemical and functional stabilization of an *ermC–cat-86* transcriptional fusion. (a) Physical map of pLS767. The plasmid contains a transcriptional fusion between *ermC*, including its promoter and leader peptide sequence, and a promoterless *cat-86* gene containing its own ribosome-binding site (SD). The *ermC* transcriptional +1 site, leader peptide translation start (M), and stop codon (*) are indicated. (b) Northern blot analysis using total RNA isolated from *B. subtilis* PSL-1(pLS767) at the times indicated after rifampin addition and a *cat-86*-specific probe. Molecular sizes of markers, 16S and 23S rRNA, are shown on the right in bases. (c) Specific activity of CAT from cells containing pLS767 grown with or without erythromycin.

containing the *ermC* promoter and leader peptide was cloned upstream of the promotorless *cat-86* gene on plasmid pPL603B (29), resulting in a transcriptional fusion carried as part of plasmid pLS767 (Fig. 7a). The decay of the hybrid transcript was analyzed by blotting. RNA isolated from *B. subtilis* containing pLS767 treated as for Fig. 2a was hybridized with a *cat-86*-specific DNA probe. The half-life of the hybrid transcript was increased by erythromycin from less than 2 min to approximately 20 min (Fig. 7b). Extracts from erythromycin-induced cells had eight-fold higher CAT activity than did uninduced cells after 90 min (Fig. 7c). Thus, unlike the *ermA-lacZ* translational fusion, the erythromycin-stabilized hybrid *ermC–cat-86* transcript appears to be functional for protein synthesis.

DISCUSSION

We studied the mechanism of erythromycin-induced stabilization of *ermA* mRNA in *B. subtilis*. Previous work (26)

suggested that erythromycin-bound ribosomes which stall while translating the first *ermA* leader peptide physically stabilize the transcript. It was further suggested that, because of the proximity of the leader peptide to the start of the transcript, a stalled ribosome would shield almost the entire 5′ end of the transcript and might thereby stabilize the mRNA by limiting the accessibility of RNases which bind at the 5′ end (3, 26). To test this model, the sequences at the 5′ end of the *ermA* transcript were systematically altered and the decay patterns of the resultant transcripts were determined. Our results support a model whereby erythromycin-bound ribosomes block the accessibility of a 5′-to-3′ processive RNase to the 5′ end of the *ermA* transcript.

Possible limitation by stalled ribosomes of nuclease binding to the 5′ end of the *ermA* transcript. To address the question of the accessibility of nucleases that bind to the 5′ end of *ermA* mRNA and the relationship to mRNA stabilization, we compared the decay of wild-type *ermA* mRNA with the decay *ermA* transcripts to which DNA sequences were added that increased the distance between the +1 site and the location of ribosome stalling. Whereas the full-length wild-type transcript was stabilized by erythromycin, only mRNA downstream from the leader region was stabilized in the extended transcripts. The sequences added upstream of the leader region, and thus not protected by a stalled ribosome, quickly decayed. Furthermore, when another leader peptide sequence was added 5′ to an elongated *ermA* transcript, the entire transcript was stabilized by erythromycin. These data are consistent with the stabilization model whereby stalled ribosomes block nuclease accessibility at the 5′ end because complete transcripts were stabilized only when ribosome stall sites were close to the +1 site.

Processive degradation of *ermA* mRNA from the 5′ end. Detection of specific decay intermediates whose 5′ ends map to the *ermA* leader region allowed us to draw further conclusions about the mechanism of *ermA* mRNA decay. Several points are relevant. (i) The ratio of decay intermediates to the full-length transcript was greater with the three extended *ermA* transcripts than with wild-type *ermA*. Because extending the mRNA 5′ to the leader region affected the concentration of decay intermediates that map to the leader region, we concluded that the intermediates are the result of processive decay from the 5′ end of the transcript rather than a result of endonucleolytic cleavage. (ii) The decay pattern of the mRNA consisting of an additional leader peptide sequence 5′ to an extended *ermA* transcript (*ermA238*) is also consistent with processive decay rather than endonucleolytic cleavage. In contrast to the simple insertion without the additional 5′ leader peptide sequence (*ermA202*), the entire *ermA238* transcript was stabilized by erythromycin. If *ermA238* mRNA was subjected to endonucleolytic cleavage, adding an additional leader peptide sequence at the 5′ end should not have stabilized the full-length transcript. (iii) The apparent precursor-product relationship of the decay intermediates observed over time is also consistent with processive decay (Fig. 3b).

Mapping of 5′ ends of decay intermediates near ribosome stall sites. The 5′ ends of the intermediates, x, y, and z, detected in the decay of *ermA* transcripts consistently mapped within the two *ermA* leader peptides. The translational-attenuation model for induction of expression of *ermA* predicts that erythromycin-bound ribosomes stall while translating these peptides. We detected these decay intermediates only in the presence of erythromycin and postulate that they are due to blockage of the progression of a 5′-to-3′ processive nuclease by erythromycin-bound ribosomes. Recent genetic (21) and biochemical (M. Mayford and B. Weisblum, EMBO J., in press) experiments with the closely related *ermC* gene have suggested that codons 5 to 9 of the *ermC* leader peptide are critical for erythromycin-induced ribosome stalling, which is thought to occur at or close to codons 8 (P site) and 9 (A site). On the basis of the amino acid homology between the *ermC* and *ermA* leader peptides, we can align *ermA* leader peptides 1 and 2 functionally with the *ermC* leader peptide and in relation to the observed cleavage sites x, y, and z (Fig. 8). It seems likely that, as in the *ermC* leader peptide, erythromycin-bound ribosomes stall in the two *ermA* leader peptides at the functionally equivalent codons, as indicated.

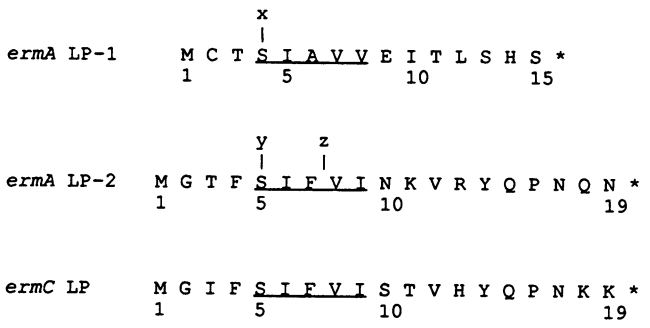

FIG. 8. Alignment of *ermA* and *ermC* leader peptide (LP) amino acid sequences.

If, as we predict, erythromycin-bound ribosomes stall midway through the *ermA* leader peptides, the 5′ ends of decay intermediates x, y, and z occur very near the P and A sites of the stalled ribosomes. Using poly(U) as a model transcript, Kang and Cantor (19) showed that in vitro ribosomes protect 20 nucleotides upstream of the P and A sites from degradation by RNase T2. In contrast, with the *ermA* transcript in vivo, the processive nuclease which produces the observed intermediates would have to penetrate the trailing edge of the ribosome.

Model of *ermA* mRNA decay. Taken together, our results suggest that the *ermA* transcript is degraded by a nuclease that binds at the 5′ end and cleaves processively toward the 3′ end. In the presence of erythromycin, the progression of the nuclease is blocked by stalled erythromycin-bound ribosomes in the two leader peptide sequences, resulting in stable decay intermediates x, y, and z. Because of the proximity of the stalled ribosome to the 5′ end of the wild-type *ermA* transcript, the nuclease would be expected to bind inefficiently, leaving a predominantly intact full-length transcript and a small amount of decay intermediates. However, the nuclease would attach efficiently to the elongated *ermA* transcripts, leading to a high concentration of decay intermediates. The stalled ribosome thus can act in either of two ways. (i) Ribosomes stalled close to the 5′ end of the transcript may prevent loading of the nuclease on the transcript, and (ii) ribosomes stalled downstream from the 5′ end of the transcript act as a barricade to further 5′-to-3′ degradation beyond the stall site. (This model of *ermA* mRNA decay is depicted schematically in Fig. 9.)

It should be noted that no 5′-to-3′ exonucleases have been found in bacteria (10). However, as suggested by King et al. (20), it is possible that transcripts may be degraded in a 5′-to-3′ direction by processive endonucleases. On the basis of our results, we cannot distinguish between a processive endonuclease that initially cleaves the mRNA several nucleotides from the 5′ end and an exonuclease that cleaves the very first residue.

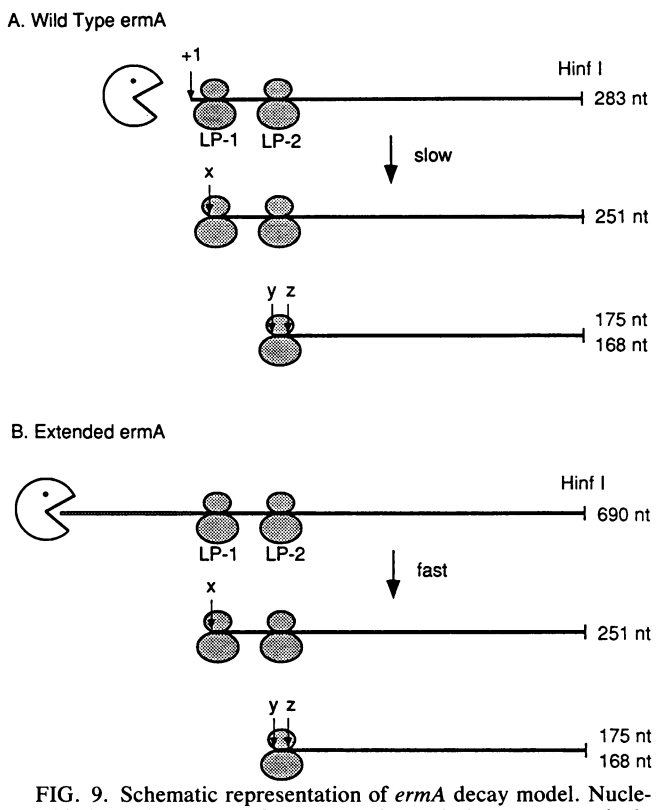

FIG. 9. Schematic representation of *ermA* decay model. Nuclease binds at the 5′ end of the transcript and cleaves processively toward the 3′ end. Erythromycin-bound ribosomes stalled in the two leader peptides (LP-1 and LP-2) block progression of the nuclease, resulting in decay intermediates x, y, and z. (A) Wild-type *ermA* transcript. Because of the proximity of the stalled ribosome to the 5′ end of the transcript, the nuclease binds inefficiently, leaving a predominantly intact full-length transcript and small amounts of intermediates x, y, and z. (B) Extended *ermA* transcript. Nuclease attaches to the transcript efficiently and degrades it rapidly to form decay intermediates x, y, and z.

Influences of 5′ ends of other transcripts on mRNA decay rates. Decay of *E. coli lacZ* transcripts by a 5′-to-3′ mechanism was proposed previously by Cannistraro et al. (8, 9). Those investigators also suggested that translating ribosomes are the limiting factor in the rate of unidirectional 5′-to-3′ decay. Although 5′-to-3′ decay has not been demonstrated for other transcripts, there are several cases in which the 5′ ends of transcripts have been shown to influence mRNA decay rates. Yamamoto and Imamoto (30) showed that the half-life of *E. coli trp* mRNA was increased 10-fold when it was transcribed from the bacteriophage lambda p_L promoter rather than from p_{trp}. Gorski et al. (12) demonstrated that the 5′ end of phage T4 gene 32 fused to the *E. coli lacZ* gene stabilized the hybrid transcript in T4-infected cells. Belasco et al. (5) examined fusions between the long-lived *E. coli ompA* gene and the short-lived *E. coli bla* gene. The decay rates of the hybrid transcripts were determined by the 5′ ends of the mRNAs, as *ompA-bla* transcripts were more stable than *bla-ompA* transcripts.

Finally, when *ompA* is transcribed from the *tac* promoter, thus extending the *ompA* transcript length by 54 nt, the half-life of *tac-ompA* mRNA is reduced 10-fold compared with that of wild-type *ompA* transcripts (22). If 5′ degradation of the *ompA* and *ermA* transcripts occurs by formally similar mechanisms, it is possible that the critical structural element of the *ompA* message which confers stability likewise prevents nuclease attachment to the 5′ end of this message. The observed reduction in *ompA* mRNA half-life as a consequence of the 54-nt extension thus may reflect the difference between the effect of a barricade which acts solely as a barrier to processive nucleolytic degradation of the message versus a barricade which, owing to its placement relative to +1, additionally retards the initial rate of attachment of the degradative nuclease to the message.

Determination of the decay rate of *cat-86* mRNA by its 5′ end. The finding that adding the sequence that encodes the *ermC* leader peptide to the 5′ end of *cat-86* mRNA stabilizes the entire fusion transcript in the presence of erythromycin (Fig. 7) suggests that the rate-limiting step in decay of *cat-86* transcripts is at the 5′ end and not endonucleolytic or at the 3′ end. Ambulos et al. (1) have noted that the *cat-86* transcript undergoes degradation at discrete positions (at least two) internal to the *cat-86* coding region by a putative endo-RNase. To reconcile these results, we assumed that either the cleavages noted by Ambulos et al. (1) are not rate limiting or the nuclease that produces the cleavages normally binds at the 5′ end of the *cat-86* transcript and then cleaves further downstream.

In our previous report (26), we noted a lack of the expected increment in expression of *lacZ* fused to *ermA* proportional to the induced increment in mRNA half-life. A similar dissociation between physical and functional stabilities was seen by Newbury et al. (24) for *hisJ* relative to its (naturally occurring) 3′-terminal REP sequence, which serves as an mRNA-stabilizing element in this system. In contrast, a direct correlation between mRNA stability and *cat* expression was seen in a *cat*-REP construction (24). These findings parallel our finding that the *ermA* leader, which confers physical stability on both *lacZ* mRNA and *cat* mRNA, appears to confer functional stability only on *cat*.

ACKNOWLEDGMENTS

We thank Mark Mayford and Stuart Peltz for critically reading the manuscript. We are grateful to Tony Chang for expert assistance in preparation of the figures and to Terry Stewart for photography.

The 19-mer oligonucleotide used for in vitro mutagenesis was synthesized by the University of Wisconsin Protein Sequence-DNA Synthesis Facility, supported by funds from the Public Health Service, National Institutes of Health (shared-equipment grant S10-RR01684, National Cancer Institute continuing support grant CA-07175, and the general research support grant to the University of Wisconsin Medical School), the National Science Foundation Biological Instrumentation Program, Division of Molecular Biosciences grant DMB-8514305, and the University of Wisconsin Graduate School. This work was supported by Public Health Service research grant AI-18283 from the National Institutes of Health.

LITERATURE CITED

1. **Ambulos, N. P., Jr., E. J. Duvall, and P. S. Lovett.** 1987. The mRNA for an inducible chloramphenicol acetyltransferase gene is cleaved into discrete fragments in *Bacillus subtilis*. J. Bacteriol. **169**:967–972.
2. **Band, L., and D. J. Henner.** 1984. *Bacillus subtilis* requires a stringent Shine-Dalgarno sequence for gene expression. DNA **3**:17–21.
3. **Bechhofer, D. H., and D. Dubnau.** 1987. Induced mRNA stability in *Bacillus subtilis*. Proc. Natl. Acad. Sci. USA **84**:498–502.
4. **Belasco, J. G., and C. F. Higgins.** 1988. Mechanisms of mRNA decay in bacteria: a perspective. Gene **72**:15–23.
5. **Belasco, J. G., G. Nilsson, A. von Gabain, and S. N. Cohen.** 1986. The stability of *E. coli* gene transcripts is dependent on determinants localized to specific mRNA segments. Cell **46**:

245–251.
6. **Berk, A. J., and P. A. Sharp.** 1977. Sizing and mapping of early adenovirus mRNAs by gel electrophoresis of S1 endonuclease digested hybrids. Cell **12**:721–732.
7. **Brawerman, G.** 1989. mRNA decay: finding the right targets. Cell **57**:9–10.
8. **Cannistraro, V. J., and D. Kennell.** 1985. Evidence that the 5′ end of *lac* mRNA starts to decay as soon as it is synthesized. J. Bacteriol. **161**:820–822.
9. **Cannistraro, V. J., M. N. Subbarao, and D. Kennell.** 1986. Specific endonucleolytic cleavage sites for decay of *Escherichia coli* mRNA. J. Mol. Biol. **192**:257–274.
10. **Deutscher, M. P.** 1985. *E. coli* RNases: making sense of alphabet soup. Cell **40**:731–732.
11. **Feinberg, A., and B. Vogelstein.** 1983. A technique for radiolabeling DNA restriction fragments to high specific activity. Anal. Biochem. **132**:6–13.
12. **Gorski, K., J.-M. Roch, P. Prentki, and H. M. Krisch.** 1985. The stability of bacteriophage T4 gene 32 mRNA: a 5′ leader sequence that can stabilize mRNA transcripts. Cell **43**:461–469.
13. **Gough, J. A., and N. E. Murray.** 1983. Sequence diversity among related genes for recognition of specific targets in DNA. J. Mol. Biol. **166**:1–19.
14. **Gryczan, T. J., G. Grandi, J. Hahn, R. Grandi, and D. Dubnau.** 1980. Conformational regulation of erythromycin-induced drug resistance. Nucleic Acids Res. **8**:6081–6097.
15. **Harwood, C. R., D. M. Williams, and P. S. Lovett.** 1983. Nucleotide sequence of a *Bacillus pumilus* gene specifying chloramphenicol acetyltransferase. Gene **24**:163–169.
16. **Horinouchi, S., and B. Weisblum.** 1980. Post-transcriptional modification of mRNA conformation: mechanism that regulates erythromycin-induced resistance. Proc. Natl. Acad. Sci. USA **77**:7079–7083.
17. **Horinouchi, S., and B. Weisblum.** 1982. Nucleotide sequence and functional map of pE194, a plasmid that specifies inducible resistance to macrolide, lincosamide, and streptogramin type B antibiotics. J. Bacteriol. **150**:804–814.
18. **Horinouchi, S., and B. Weisblum.** 1982. Nucleotide sequence and functional map of pC194, a plasmid that specifies inducible chloramphenicol resistance. J. Bacteriol. **150**:815–825.
19. **Kang, C., and C. R. Cantor.** 1985. Structure of ribosome-bound messenger RNA as revealed by enzymatic accessibility studies. J. Mol. Biol. **181**:241–251.
20. **King, T. C., R. Sirdeskmukh, and D. Schlessinger.** 1986. Nucleolytic processing of ribonucleic acid transcripts in procaryotes. Microbiol. Rev. **50**:428–451.
21. **Mayford, M., and B. Weisblum.** 1989. *ermC* leader peptide: amino acid sequence critical for induction by translational attenuation. J. Mol. Biol. **206**:69–79.
22. **Melefors, O., and A. von Gabain.** 1988. Site-specific endonucleolytic cleavages and the regulation of stability of *E. coli ompA* mRNA. Cell **52**:893–901.
23. **Murphy, E.** 1985. Nucleotide sequence of *ermA*, a macrolide-lincosamide-streptogramin B determinant in *Staphylococcus aureus*. J. Bacteriol. **162**:633–640.
24. **Newbury, S. F., N. H. Smith, E. C. Robinson, I. D. Hiles, and C. F. Higgins.** 1987. Stabilization of translationally active mRNA by prokaryotic REP sequences. Cell **48**:297–310.
25. **Ostroff, G. R., and J. J. Pène.** 1983. Molecular cloning with bifunctional plasmid vectors in *Bacillus subtilis*: isolation of a spontaneous mutant of *Bacillus subtilis* with enhanced transformability for *Escherichia coli*-propagated chimeric plasmid DNA. J. Bacteriol. **156**:934–936.
26. **Sandler, P., and B. Weisblum.** 1988. Erythromycin-induced stabilization of *ermA* messenger RNA in *Staphylococcus aureus* and *Bacillus subtilis*. J. Mol. Biol. **203**:905–915.
27. **Shaw, W. V.** 1975. Chloramphenicol acetyltransferase from chloramphenicol-resistant bacteria. Methods Enzymol. **43**:737–755.
28. **Weisblum, B., C. Siddhikol, C.-J. Lai, and V. Demohn.** 1971. Erythromycin-inducible resistance in *Staphylococcus aureus*: requirements for induction. J. Bacteriol. **106**:835–847.
29. **Williams, D. M., E. J. Duvall, and P. S. Lovett.** 1981. Cloning restriction fragments that promote expression of a gene in *Bacillus subtilis*. J. Bacteriol. **146**:1162–1165.
30. **Yamamoto, T., and F. Imamoto.** 1975. Differential stability of *trp* messenger RNA synthesized originating at the *trp* promoter and p_L promoter of lambda *trp* phage. J. Mol. Biol. **92**:289–309.
31. **Zoller, M. J., and M. Smith.** 1983. Oligonucleotide-directed mutagenesis of DNA fragments cloned into M13 vectors. Methods Enzymol. **100**:468–500.